Space Sci Rev (2010) 152: 565–590
DOI 10.1007/s11214-009-9553-2

Dynamo Scaling Laws and Applications to the Planets

U.R. Christensen

Received: 6 February 2009 / Accepted: 8 June 2009 / Published online: 7 July 2009

Abstract Scaling laws for planetary dynamos relate the characteristic magnetic field strength, characteristic flow velocity and other properties to primary quantities such as core size, rotation rate, electrical conductivity and heat flux. Many different scaling laws have been proposed, often relying on the assumption of a balance of Coriolis force and Lorentz force in the dynamo. Their theoretical foundation is reviewed. The advent of direct numerical simulations of planetary dynamos and the ability to perform them for a sufficiently wide range of control parameters allows to test the scaling laws. The results support a magnetic field scaling that is not based on a force balance, but on the energy flux available to balance ohmic dissipation. In its simplest form, it predicts a field strength that is independent of rotation rate and electrical conductivity and proportional to the cubic root of the available energy flux. However, rotation rate controls whether the magnetic field is dipolar or multipolar. Scaling laws for velocity, heat transfer and ohmic dissipation are also discussed. The predictions of the energy-based scaling law agree well with the observed field strength of Earth and Jupiter, but for other planets they are more difficult to test or special pleading is required to explain their field strength. The scaling law also explains the very high field strength of rapidly rotating low-mass stars, which supports its rather general validity.

Keywords Planetary magnetic fields · Geodynamo · Dynamo models

1 Introduction

The observed magnetic field strength B_p at the surface of those planets in the solar system that have presently an active dynamo varies over a wide range, from approximately 400 nT at Mercury to 500,000 nT at Jupiter. For the dipole moment, which is given by $M \approx B_p R_p^3$ for a dominantly dipolar field with R_p the planetary radius, the range is even larger, between 4×10^{12} Tm^3 (Mercury) and 1.5×10^{20} Tm^{-3} (Jupiter). The primary aim of a dynamo scaling theory is to explain the field strength in terms of fundamental properties of the planet

U.R. Christensen (✉)
Max-Planck-Institut für Sonnensystemforschung, 37191 Katlenburg-Lindau, Germany
e-mail: christensen@mps.mpg.de

Table 1 Proposed scaling laws

#	Rule	Author	Remark
1	$B_p R_p^3 \propto (\rho\Omega R_p^5)^a$	e.g. Russell (1978)	magnetic Bode law
2	$B^2 \propto \rho\Omega^2 R_c^2$	Busse (1976)	
3	$B^2 \propto \rho\Omega\sigma^{-1}$	Stevenson (1979)	Elsasser number rule
4	$B^2 \propto \rho R_c^3 q_c \sigma$	Stevenson (1984)	at low energy flux
5	$B^2 \propto \rho\Omega R_c^{5/3} q_c^{1/3}$	Curtis and Ness (1986, modified)	mixing length theory
6	$B^2 \propto \rho\Omega^{3/2} R_c \sigma^{-1/2}$	Mizutani et al. (1992)	
7	$B^2 \propto \rho\Omega^2 R_c$	Sano (1993)	
8	$B^2 \propto \rho\Omega^{1/2} R_c^{3/2} q_c^{1/2}$	Starchenko and Jones (2002)	MAC balance
9	$B^2 \propto \rho R_c^{4/3} q_c^{2/3}$	Christensen and Aubert (2006)	energy flux scaling

or its dynamo region. It is not immediately obvious which quantities play the key role, but candidates are the radius R_c of the electrically conducting fluid core of the planet, the conductivity σ and density ρ of the core, the rotation rate Ω and the convected energy flux q_c in the core. Also, it is not clear if a single scaling law is applicable to all magnetic planets. This may require that their dynamos are qualitatively similar and differ only in specific parameter values. As we will see, there are probably sufficiently severe differences between planetary dynamos so that the application of the same scaling law to all of them is not straightforward.

The interest in a scaling theory for planetary magnetic fields is twofold. In terms of the theoretical understanding of planetary magnetism, a well-established scaling law is an essential part of a comprehensive dynamo theory. On the more practical side, such a law would allow to make predictions for the paleo-fields of the solar system planets, at times when control parameters (e.g. q_c, Ω) had been different and when now extinct dynamos were active in Mars or other planetary bodies. This has possible applications to the question of atmospheric evolution and planetary habitability (Dehant et al. 2007).

Over the past decades space missions provided data on the first-order magnetic field properties of the planets. At the same time, scaling laws for their field strength have been proposed with a rather confusing diversity (Table 1). The 'magnetic Bode law' (#1 in the Table 1), suggesting a relation between the magnetic dipole moment and the angular momentum of the planet, is purely empirical. Most other scaling laws are based on an assumed force balance between Coriolis force and Lorentz force, but make different assumptions on the characteristic velocity or length scales in the dynamo. Rules #4 and #9 in Table 1 consider the energy flux that is available to balance ohmic dissipation.

In Table 1, B usually refers to the characteristic magnetic field strength inside the dynamo. It is assumed that the strength of the exterior dipole field is proportional to B. The predictions of the proposed scaling laws have been compared with the observed planetary fields and fair or good agreement has been claimed in every case. Given the diversity of the scaling laws, it seems quite surprising that they all fit the observations more or less well. One reason is that in many cases the comparison has been made in terms of the dipole moment, which means that the predicted field strength is multiplied by the cube of the radius. The pitfalls of such a procedure has been discussed by Cain et al. (1995) for the case of the magnetic Bode law. Suppose that for a set of hypothetical planets the surface field strength B_p is uncorrelated with ρ, Ω and R_p, and that all these quantities vary within some range. When B_p is multiplied by R_p^3 and $\rho\Omega$ is multiplied by R_p^5 to obtain the magnetic moment and the angular momentum, respectively, a correlation is found between the logarithms of

the two moments (with a most probable exponent $a = 3/5$ in Table 1). Obviously this has no physical basis other than that big planets are more likely than small planets to have large values in properties that depend on high powers of the radius.

A new perspective on planetary scaling laws has been opened by the advent of numerical dynamo models (Glatzmaier and Roberts 1995; Christensen and Wicht 2007). The ability to run simulations for a large number of model cases that cover a substantial range of the values of control parameters allows to test scaling laws against the numerical results. One point of concern is that in these models the viscosity and the thermal diffusivity are far larger than they are in planetary cores and, therefore, the models may be in a different dynamical regime.

This paper has three main sections. In the next one various theoretical approaches for scaling laws are discussed. In Sect. 3 theoretical predictions are compared with the results from numerical dynamo models. The emphasis is on scaling laws of magnetic field strength, but we also address the scaling of velocity and the rate of ohmic dissipation. Also, the question of what controls the magnetic field morphology is of interest. In Sect. 4 the scaling laws are compared with the known magnetic properties of solar system planets and also with observational data for certain classes of stars.

2 Theory

Before considering principles for scaling laws, some fundamental requirements and assumptions for planetary dynamos are reiterated. A fluid region of sufficient thickness D with a sufficiently high electrical conductivity σ must exist inside the planet. The fluid must move with a sufficiently large velocity U, so that the magnetic Reynolds number

$$Rm = \frac{U D}{\lambda} \tag{1}$$

exceeds a critical value Rm_{crit} ($\lambda = 1/\mu_o\sigma$ is the magnetic diffusivity). The flow pattern must also be suitable for dynamo action, which requires a certain complexity. Although dynamos may also exist for flows that are excited by precession or by tides (Wicht and Tilgner 2009, this issue), we assume here an origin by thermal or compositional buoyancy forces. Also, we take a spherical shell geometry for the dynamo region and assume that Coriolis forces play a significant part in the force balance of the fluid and influence the pattern of convection. With these assumptions the requirement for 'flow complexity' seems to be satisfied and self-sustained dynamo action is possible above $Rm_{crit} \approx 50$ (Christensen and Aubert 2006). We will also assume that the fluid can be treated as incompressible (Boussinesq approximation), although modifications that apply to the case of strong density stratification are also discussed.

2.1 Magnetostrophic Force Balance

The equation of motion for an incompressible, rotating and electrically conducting fluid driven by thermal buoyancy in the presence of a magnetic field is (Gubbins and Roberts 1987):

$$\rho\left(\frac{\partial \mathbf{u}}{\partial t} + (\mathbf{u}\cdot\nabla)\mathbf{u}\right) + 2\rho\Omega\mathbf{e}_z \times \mathbf{u} + \nabla P = \rho\nu\nabla^2\mathbf{u} + \rho\alpha g T\mathbf{e}_\mathbf{r} + \mathbf{j}\times\mathbf{B}, \tag{2}$$

where $\mathbf{u}$ is velocity, Ω rotation rate, ρ density, P non-hydrostatic pressure, ν kinematic viscosity, α thermal expansivity, g gravity, T temperature, $\mathbf{B}$ magnetic field, $\mathbf{j} = \mu_o^{-1} \nabla \times \mathbf{B}$ current density, r radius and z the direction parallel to the rotation axis. The terms in Eq. 2 describe in order the linear and non-linear parts of inertial forces, Coriolis force, pressure gradient force, viscous force, buoyancy force and Lorentz force.

A very simple estimate for the relative magnitude of the various forces in the Earth's core is obtained by assuming the following characteristic values (in SI-units): $U \approx 10^{-4}$, $\Omega \approx 7 \times 10^{-5}$, $\rho \approx 10^4$, $B \approx 5 \times 10^{-3}$, and for the characteristic length scale associated with the various spatial derivatives $\ell \approx 3 \times 10^5$. The viscous force and the inertial force turn out to be much smaller than the Lorentz force and the Coriolis force, whose magnitudes are comparable (magnetostrophic balance). The magnitude of temperature anomalies driving the flow is hard to estimate *a priori*, but it is assumed that buoyancy also contributes at leading order. The resulting force balance is called the MAC-balance (from **M**agnetic, **A**rchimedean and **C**oriolis forces).

One of the simplest scaling rules for the magnetic field based on the magnetostrophic force balance is the Elsasser number rule. In order to derive it, we relate the characteristic current density J in the Lorentz force term in Eq. 2 to the characteristic velocity U by the generalized Ohm's law, $\mathbf{j} = \sigma(\mathbf{E} + \mathbf{u} \times \mathbf{B})$. Ignoring the electric field $\mathbf{E}$, this results in $J \propto \sigma U B$ and the order of the Lorentz force is $JB \propto \sigma U B^2$, while that of the Coriolis force is $2\rho\Omega U$. Their ratio is the Elsasser number, in which the velocity drops out:

$$\Lambda = \frac{\sigma B^2}{2\rho\Omega}. \tag{3}$$

Since both forces are assumed to be of the same order, the Elsasser number should be of order one, which leads to the prediction for the magnetic field strength given by rule #3 in Table 1. The Elsasser number rule is supported by the theory of rotating magnetoconvection, i.e. convection in an imposed magnetic field. Convection is inhibited both by rotational effects and by magnetic effects when they are considered in isolation. However, for an imposed field of simple geometry it has been shown that the combination of both effects will actually reduce the impeding influence and that this constructive interplay is most efficient when the Elsasser number is around one (Chandrasekhar 1961; Stevenson 1979). Applied to dynamos, it is argued that as long as the magnetic field is weak ($\Lambda \ll 1$), any field growth will intensify convection, meaning more efficient dynamo action and further increase of the field. Field growth at $\Lambda \gg 1$ would weaken convection, hence it is assumed that the field equilibrates at an Elsasser number of one.

The Elsasser rule has found widespread acceptance because of its plausible theoretical basis and because reasonable estimates of the magnetic field strength in the cores of the Earth and some other planets put the Elsasser number in the range of 0.1–10 (Stevenson 2003). Possible caveats are: (1) The effect on convection of the complex magnetic field that might be expected in a dynamo could be different from that of the simple field assumed in magnetoconvection. (2) The assumption $J \propto UB$ may not hold because velocity and magnetic field could be largely aligned with each other. (3) The Coriolis forces could be balanced to a large degree by a pressure gradient force (nearly geostrophic flow) and only the residual must be balanced by electromagnetic or other forces. Furthermore, Stevenson (1983, 1984) pointed out that the Elsasser number rule (as well as several other proposed scaling laws) ignore the energy requirement for maintaining a magnetic field against ohmic dissipation. He suggested that the Elsasser number rule is only applicable when sufficient energy is available.

Other scaling rules based on a magnetostrophic force balance (#2,5,6,7 in Table 1) have been derived by expressing the current density in the Lorentz force term by the curl of **B** and by assuming a characteristic length scale for the field ℓ_B. Often $\ell_B \approx R_c$ is set. This gives the order of the Lorentz force as $\mu_o^{-1} B^2 R_c^{-1}$. Balancing it with the Coriolis force one obtains

$$B^2 \propto \mu_o \rho U \Omega R_c. \tag{4}$$

The choice of R_c for ℓ_B is certainly too large, and Starchenko and Jones (2002) assume it to be 0.02 R_c. But as long as ℓ_B is a fixed fraction of R_c, this will only affect the prefactor in the scaling law. A weak point is that we have no particular reason to assume ℓ_B to be constant. Typically it should vary with the magnetic Reynolds number as $\ell_B / R_c \propto Rm^{-1/2}$ (e.g. Galloway et al. 1978), although Starchenko and Jones (2002) argue that for large Rm the magnetic length scale may approach a constant value. A scaling rule for the velocity U is needed in order to obtain from Eq. 4 a law that relates the magnetic field to the fundamental physical quantities. In some cases, e.g. rule #6 in Table 1, an educated guess had been made, but in other cases the estimate for U has been based on some scaling theory or other. This will be addressed in the next section.

2.2 Velocity Scaling

We will consider three different scaling rules for the characteristic velocity U, based on force balance arguments: Mixing length theory, a MAC-balance estimate, and an estimate based on the triple force balance Coriolis force, inertia, and buoyancy.

The mixing length theory is frequently applied for highly turbulent convection in stars (Kippenhahn and Weigert 1990). Assuming a characteristic length scale ℓ on which convective mixing of momentum and entropy (or temperature in the Boussinesq limit) occur, and balancing the nonlinear inertia term and the buoyancy term in Eq. 2, results in $\rho U^2/\ell \propto \rho \alpha g T'$, where T' stands for the characteristic temperature fluctuations away from the radially averaged temperature distribution. In convection upwelling and downwelling flow are positively correlated with positive and negative values of T', respectively, hence the convected heat flux can be written as $q_c \propto \rho c_p U T'$, where c_p is the specific heat capacity. Introducing the temperature scale height $H_T = c_p/(\alpha g)$, the velocity scales as

$$U \propto \left(\frac{\ell q_c}{\rho H_T} \right)^{1/3}. \tag{5}$$

Note that the temperature scale height does not enter because the adiabatic temperature lapse would be of interest *per se*, but because the ratio ℓ / H_T describes the thermodynamic efficiency of the conversion of heat into kinetic energy through the work done by buoyancy forces. In stellar theory it is usually assumed that the mixing length ℓ is of the order of the pressure (or density) scale height. In planets the core radius R_c or the depth of the convection layer D are taken for ℓ, because here they are smaller than the density scale height (Stevenson 2003). Combining Eqs. 4 and 5 results in the magnetic field scaling rule suggested by Curtis and Ness (1986) when H_T is fixed. When we take into account that for fixed α and c_p gravity and H_T^{-1} scale as $\rho_c R_c$, we obtain rule #5 in Table 1. A caveat against this rule is that planetary dynamos are probably not in a regime described by a mixing length balance, where the energy generated by the work of buoyancy forces is transported through an inertial cascade to small length scales where viscous dissipation kicks in.

In the MAC balance regime the buoyancy forces do work against Lorentz forces and generate magnetic energy. Because the Lorentz force is assumed to be of the same order as

the Coriolis force, we can balance the latter against buoyancy forces (Starchenko and Jones 2002), i.e. $\rho\Omega U \propto \rho g \alpha T'$, and obtain

$$U \propto \left(\frac{q_c}{\rho \Omega H_T} \right)^{1/2}. \tag{6}$$

Inserting this into Eq. 4 and using $H_T^{-1} \propto \rho R_c$ leads to rule #7 in Table 1.

In rapidly rotating convection the flow is organized in quasi-geostrophic columns that run parallel to the rotation axis through the entire fluid shell. The Coriolis force is balanced to a large degree by the pressure gradient and the fraction that must be balanced by other forces could be much smaller than $\rho\Omega U$. Using a vorticity equation, which is obtained by applying the curl to Eq. 2, eliminates pressure forces. In the Boussinesq case the non-linear inertia term, Coriolis force term and the buoyancy term are, in this order, $\rho\nabla \times (\mathbf{u} \times (\nabla \times \mathbf{u}))$, $2\rho\Omega\partial\mathbf{u}/\partial z$, and $\rho\alpha g \nabla \times T\mathbf{e}_r$, where $\nabla \times \mathbf{u}$ is vorticity and $\mathbf{e}_r$ the radial unit vector. Aubert et al. (2001) considered a balance between these three terms in the vorticity equation (CIA-balance from **C**oriolis, **I**nertia, **A**rchimedean). The characteristic length scale ℓ associated with the differential operators in the inertial term and in the buoyancy term is assumed to be the same. Typically $\ell \ll R_c$, whereas a much larger scale L is associated with the z-derivative in the Coriolis term because of the quasi-geostrophic flow structure. ℓ must not be assumed, unlike in mixing length theory. The triple balance provides two conditions, which allows to derive scaling rules both for U and for ℓ:

$$U \propto \left(\frac{q_c}{\rho H_T} \right)^{2/5} \left(\frac{L}{\Omega} \right)^{1/5}, \tag{7}$$

$$\ell \propto \left(\frac{UL}{\Omega} \right)^{1/2}. \tag{8}$$

In the Boussinesq case we can set $L \approx R_c$, but we note here that in the case of density stratification the Coriolis term in the vorticity equation is modified, which implies that the length scale L is then of the order of the density scale height H_ρ. Equation 7 fits the convection velocity found in laboratory experiments (Aubert et al. 2001) and numerical simulations (Christensen 2002) of rapidly rotating convection. But it is less clear if it applies to magnetohydrodynamic flow, where according to the usual assumption Lorentz forces replace the inertial forces as a leading-order contributor to the force balance and might lead to a break-up of the quasi-geostrophic flow structure.

2.3 Power-Based Magnetic Field Scaling

Aside from satisfying the relevant force balance, any dynamo must be thermodynamically consistent. In particular, the ohmic dissipation associated with a magnetic field of certain strength and geometry cannot exceed that part of the energy flux that is available for conversion to other forms of energy. A discussion of basic principles of the energetics of Earth's core can be found in Breuer et al. (2009, this issue). For estimating the variation of magnetic field strength during the evolutionary history of a planet, Stevenson et al. (1983) assumed a linear dependence of B^2 on the energy flux. Stevenson (1984) suggested that in cases of a comparatively low energy flux, the available energy limits the magnetic field strength to values that correspond to an Elsasser number $\Lambda < 1$, whereas at high flux the field saturates at $\Lambda \approx 1$. His prediction for the low-flux regime results in rule #4 in Table 1. Based on concepts laid down in Stacey (1977),

Schubert et al. (1988) arrived at basically the same rule, which was applied to model the evolution of Mercury's magnetic field and in later papers (Schubert and Spohn 1990; Leweling and Spohn 1997) that of Mars. From numerical dynamo simulations Christensen and Aubert (2006) conclude that the energy flux controls the field strength in a wide range of fluxes, however, they arrive at a different dependence of field strength on heat flux and conductivity (rule # 9).

The thermodynamically available power per unit volume is q_c/H_T and the ohmic dissipation is $D = (\nabla \times \mathbf{B})^2/(\sigma\mu_o^2) \propto \lambda B^2/(2\mu_o \ell_B^2)$. When f_{ohm} is the fraction of the available power that is converted to magnetic energy and eventually lost by ohmic dissipation, the magnetic energy density $E_m = B^2/(2\mu_o)$ in the dynamo scales as

$$\frac{B^2}{2\mu_o} \propto f_{ohm} \frac{\ell_B^2}{\lambda} \frac{q_c}{H_T}. \tag{9}$$

ℓ_B^2/λ is equivalent to the ohmic dissipation time $\tau_\lambda = E_m/D$. Christensen and Aubert (2006) assume that τ_λ scales with the magnetic Reynolds number as

$$\tau_\lambda \propto L^2/\lambda Rm^{-1} = L/U. \tag{10}$$

Here, L is again the relevant 'large' length scale (R_c for planetary applications). We can now use some scaling law for the velocity to obtain the magnetic field scaling. The mixing length rule (Eq. 5) results in a particularly simple magnetic field scaling

$$\frac{B^2}{2\mu_o} \propto f_{ohm} \rho^{1/3} \left(\frac{q_c L}{H_T} \right)^{2/3}, \tag{11}$$

which leads to rule #9 in Table 1 when setting $L = R_c$ and $H_T^{-1} \propto \rho R_c$. What makes this scaling law unique is that it depends neither on the rotation rate, nor on the electrical conductivity. Using instead of the mixing length velocity the prediction from the MAC-balance or the CIA-theory, we obtain, respectively,

$$\frac{B^2}{2\mu_o} \propto f_{ohm} L \left(\frac{\rho \Omega q_c}{H_T} \right)^{1/2} \tag{12}$$

i.e. rule #8, or

$$\frac{B^2}{2\mu_o} \propto f_{ohm} \rho^{2/5} \Omega^{1/5} L^{4/5} \left(\frac{q_c}{H_T} \right)^{3/5}. \tag{13}$$

Aside from a somewhat weaker dependence on the energy flux than in Eq. 11, they predict a weak dependence (Eq. 13) or moderate dependence (Eq. 12) on the rotation rate.

The convected energy flux q_c and the temperature scale height H_T are not constant with radius in a planetary dynamo. Also, for Jupiter the radial variation of ρ can perhaps not be neglected. When the density stratification is strong (as its is in stars) the density scale height is a more appropriate measure for L than the radius of the dynamo region. Christensen et al. (2009) assume that a representative magnetic field strength is obtained by averaging Eq. 11 over the shell volume V. By introducing a reference value q_o for the heat flux (the flux at the outer boundary of the dynamo) and by normalizing density with its mean value $\bar{\rho}$, they condense the averaging of radially variable properties into an efficiency factor

$$F^{2/3} = \frac{1}{V} \int_{r_i}^{R} \left(\frac{q_c(r)}{q_o} \frac{L(r)}{H_T(r)} \right)^{2/3} \left(\frac{\rho(r)}{\bar{\rho}} \right)^{1/3} 4\pi r^2 dr, \tag{14}$$

where r_i is the inner radius of the spherical shell and $L = \min(D, H_\rho(r))$ is assumed. F is found to be of order one for a wide class of objects from planets to stars (Christensen et al. 2009). The scaling law (Eq. 11) now becomes

$$\frac{B^2}{2\mu_o} = c f_{ohm} \bar{\rho}^{1/3} (F q_o)^{2/3}, \tag{15}$$

where c is a constant prefactor.

When convection is partly driven by compositional rather than by thermal buoyancy, q_c / H_T must be augmented by the work done by the chemical flux in an appropriate way. In order to keep the formalism simple, Christensen et al. (2009, online supplementary information) replace the compositional flux by an equivalent effective convected heat flux.

3 Scaling Laws Versus Model Results

In this section the proposed scaling laws will be compared with the results of direct numerical simulations of convection-driven dynamos in rotating spherical shells. In these models the equation of motion together with the magnetic induction equation and an equation for the advection and diffusion of heat (or light element concentration) are solved, subject to appropriate boundary conditions (Christensen and Wicht 2007; Wicht and Tilgner 2009).

A rather large data basis of dynamo model results has been built over time by the author and coworkers (Christensen et al. 1999, 2009; Christensen and Tilgner 2004; Christensen and Aubert 2006). The data set is homogeneous in the sense that the basic model is simple and the same in all simulations, with driving of convection by a fixed temperature contrast ΔT between the inner and the outer boundaries of a rotating spherical shell, no-slip boundary conditions and a fixed ratio of inner boundary radius to outer boundary radius of 0.35. In Christensen et al. (2009) models with different thermal boundary conditions, meant to represent a proxy for compositional convection, are also included. The parameters describing rotation rate, viscosity, magnetic and thermal diffusivity and convective driving are varied within a fairly wide range. All the simulations have been run for a sufficient time to reach an equilibrated state. The time-averaged *rms*-values of velocity and magnetic field strength have been calculated for the equilibrium state and are taken for the characteristic values U and B. Averages of other values of interest, for example f_{ohm}, have also been recorded.

The model results have been calculated in terms of non-dimensional quantities. Non-dimensionalizing the governing equations results in a set of four control parameters.
The Ekman number describes the ratio of viscous forces to Coriolis forces

$$E = \frac{\nu}{\Omega D^2}. \tag{16}$$

The modified Rayleigh number is the ratio of driving buoyancy to retarding rotational forces

$$Ra^* = \frac{\alpha g_o \Delta T}{\Omega^2 D}. \tag{17}$$

The Prandtl number is the ratio of viscosity to thermal diffusivity κ,

$$Pr = \frac{\nu}{\kappa}, \tag{18}$$

and the magnetic Prandtl number is

$$Pm = \frac{\nu}{\lambda}. \tag{19}$$

We note that none of the scaling laws discussed so far predicts a dependence on viscosity ν or thermal diffusivity κ. In order to test them, the definition of the Rayleigh number in Eq. 17, which does not contain any diffusivity (viscosity being also subsumed under this term), is therefore more advantageous than the conventional definition $Ra = \alpha g_o \Delta T D^3/(\kappa\nu)$. The two Rayleigh numbers are related by $Ra^* = RaE^2Pr^{-1}$. Because there are three different diffusion constants in the dynamo equations, ν, κ and λ, the other three control parameters must necessarily contain diffusivities.

The scaling laws discussed above have been formulated in terms of the convected heat flux q_c, for which decent estimates exist for several planets, whereas the driving (superadiabatic) temperature contrast ΔT is unknown. Christensen and Aubert (2006) therefore introduce a flux Rayleigh number, given by $Ra_Q^* = Ra(Nu-1)E^3Pr^{-2}$, which is likewise independent of viscosity and diffusivities. The Nusselt number Nu is the ratio of heat flux in the convecting state to the conductive heat flux. Unless when flux boundary conditions are used, Ra_Q^* is therefore not a primary parameter, but is derived from the solution. The flux Rayleigh number is proportional to a non-dimensional form of the available energy flux (or convective power). For different driving modes the constant of proportionality is different. Therefore, Christensen et al. (2009) use instead of a Rayleigh number a related parameter that is directly equivalent to the available energy flux (see also Aubert et al. 2009):

$$Fq^* = \frac{Fq_o}{\rho\Omega^3 R_c^3}. \tag{20}$$

Here, F is the efficiency factor defined by Eq. 14 and q_o is the reference value of the heat flux. For Boussinesq models with $r_i/R = 0.35$ and fixed ΔT the integration of Eq. 14 leads to $F = 0.88R_c/H_T^o$ when taking for q_o the heat flux on the outer boundary (H_T^o is calculated with gravity g_o at R_c). In cases of a fixed flux q_i on the inner boundary and zero flux on the outer boundary, which is a proxy for composition convection, $F = 0.45R_c/H_T^o$ when setting the reference flux to $q_o = q_i r_i^2/R_c^2$. In both cases the heat flux must be corrected for the non-convected part, by multiplying it with $(Nu-1)/Nu$ in the Boussinesq case.

Below we will take the non-dimensional form of the available heat flux Fq^* as control parameter, and an equivalent non-dimensional form of the velocity and the magnetic field strength, to compare the various proposed scaling laws with the numerical results.

3.1 Velocity Scaling

The appropriate nondimensional form for expressing the velocity is the Rossby number

$$Ro = \frac{U}{\Omega R_c}. \tag{21}$$

In terms of the Rossby number and the non-dimensional available heat flux, the three scaling laws for the velocity discussed in Sect. 2.2 can all be written in the form

$$Ro \propto (Fq^*)^\alpha, \tag{22}$$

where the exponent α is $1/3$ in case of the mixing length scaling, $2/5$ for the CIA-balance scaling and $1/2$ for the MAC-balance scaling.

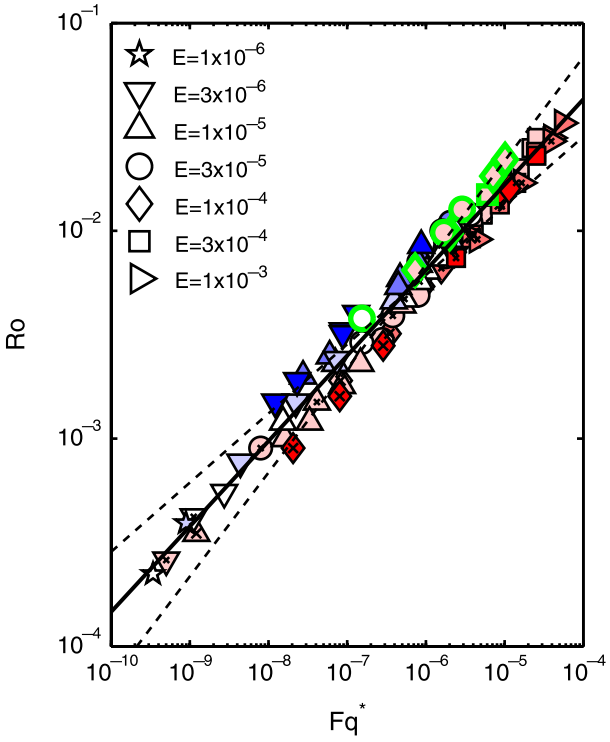

Fig. 1 Rossby number versus available power for dynamos models with dipole dominated magnetic field. *Pm* is color-coded (*dark blue* $Pm \leq 0.1$, *white* $Pm = 1$, *dark red* $Pm \geq 10$, paler shading for intermediate values). $Pr = 1$, except where indicated by a *cross* ($Pr > 1$) or circle ($Pr < 1$) inside main symbol. Black-edged symbols are for fixed ΔT, green-edged symbols for fixed heat flux at r_i and zero flux at R_c. Slopes of broken lines are 1/3 and 1/2, respectively, for the best-fitting line it is 0.411. The preexponential constant is 1.23 (1.05 for a fit with a forced exponent of 0.400)

In Fig. 1 the Rossby number is plotted versus Fq^* for the numerical model results. Here we restrict the data set to dynamos that generate a dipole dominated magnetic field, meaning that the dipole field strength on the outer boundary is at least 35% of the combined field strength in harmonic degrees 1–12. Also, only dynamos with a Nusselt number $Nu > 2$ are plotted, to exclude cases in which convection is not fully developed.

The data are well fitted by Eq. 22. Result for different values of the Ekman number and the two Prandtl numbers are collapsed on a single line. These are the parameters that involve the viscosity and diffusivities, therefore they do not play a first-order role in the dynamo models. Only with respect to the magnetic Prandtl number a slight bias seems to exist in the fit (see Christensen and Aubert 2006). The fitting exponent of 0.41 agrees best with the prediction from the CIA-balance. The lines with slopes of 1/3 and 1/2 show clear systematic deviations.

3.2 Magnetic Energy Scaling

The appropriate form of the non-dimensional magnetic energy is given by

$$E_m^* = \frac{E_m}{\rho \Omega^2 R_c^2}. \tag{23}$$

E_m^* is proportional to the squared Lorentz number defined by Christensen and Aubert (2006) for measuring magnetic field strength. The non-dimensional form of Eqs. 11–13 is

$$E_m^* = c f_{ohm} (Fq^*)^{\alpha}, \tag{24}$$

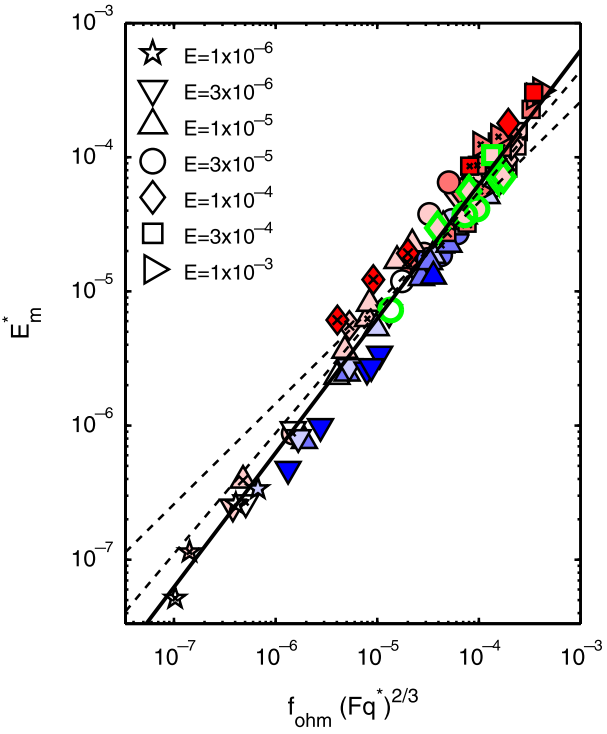

Fig. 2 Non-dimensional magnetic energy density versus available power for dynamos models with dipole-dominated magnetic field. See Fig. 1 for explanation of symbols. The slope of the fitting line has been set to 1.0, the best-fitting pre-factor is $c = 0.63$. The two broken lines refer to exponents α in Eq. 24 of 0.6 and 0.5, respectively

where the exponent α is 2/3 for the mixing-length prediction, 0.5 for the MAC-balance prediction and 0.6 for the prediction assuming a CIA-balance. In Fig. 2 we plot the magnetic energy against the right-hand side of Eq. 24, setting $\alpha = 2/3$. The best-fitting exponent for the energy flux is 0.677 (the slope in the figure has been set to one). The good fit strongly supports the scaling law Eq. 11, in which the magnetic field strength is independent of rotation rate. An exponent $\alpha = 0.6$ appears marginally compatible with the numerical results, but $\alpha = 0.5$, which corresponds to rule #8 in Table 1, is ruled out. Again, the fact that data for different values of the Ekman number and the Prandtl number are collapsed on a single line shows that diffusivities do not play a first-order role in the numerical dynamos. A weak dependence on the magnetic Prandtl number is found again—cases with high *Pm* (red symbols in Fig. 2) tend to plot slightly above the fitting line and those with low *Pm* (blue symbols) tend to plot below the line.

Although a 2/3-power law for the magnetic energy seems to be well established by the model results, we note a discrepancy—Eq. 11 has been derived using the 1/3-power law dependence of velocity on the available energy flux, whereas the numerical results clearly support a 2/5-power law (Sect. 3.1). Takahashi et al. (2008) confirmed for independent dynamo simulations in a similar parameter range the 2/5-power law for the velocity and the 2/3-power law for the magnetic energy. In Sect. 3.5 the apparent discrepancy between velocity scaling and field scaling will be discussed further.

3.2.1 Different Non-Dimensionalization Schemes and Test of Other Rules

The non-dimensionalization of magnetic energy and of convected heat flux used in the previous section (Eqs. 20 and 23) is not unique. The scales involve the square and the cube of the

rotation frequency Ω, which does not affect the magnetic field strength according to Eq. 15. Therefore, one may suspect that the good agreement in Fig. 2 is at least partly feigned, similar to the case of the 'magnetic Bode law' discussed in the introduction. To test this, different schemes for making Eq. 15 non-dimensional are explored. This also offers the opportunity to directly test other proposed magnetic field scaling rules listed in Table 1.

Dimensional analysis shows that the most general form of an energy density scale is given by

$$E_m^{scale} = \rho \Omega^p \nu^q \lambda^r \kappa^s R^{2p-2}, \tag{25}$$

with the corresponding scale for the available heat flux being

$$q^{scale} = \rho \Omega^{3p/2} \nu^{3q/2} \lambda^{3r/2} \kappa^{3s/2} R^{3p-3}. \tag{26}$$

The exponents must satisfy $p + q + r + s = 2$, but are otherwise arbitrary. In Sect. 3.2 the scaling $(p, q, r, s) = (2, 0, 0, 0)$ had been used ('rotational' scaling). In Fig. 3 four other options are shown. The different schemes of non-dimensionalizing re-shuffle the data points, but they are always decently fit by a line with slope one (fixed to this value in the plots in accord with Eq. 15). Slightly different slopes marginally improve the fits. In Fig. 3a 'magnetic scaling' is used, i.e. magnetic energy density is non-dimensionalized with $\rho\lambda^2 R^2$. This may suffer from the same caveat as the rotational scaling, because the variables are normalized with the second and third power of λ, which does not appear naturally in the scaling law. For the scaling in Fig. 3b the non-dimensional magnetic energy density is just equal to the Elsasser number Λ. It varies over three orders of magnitude, showing that the assumption $\Lambda \approx 1$ (rule #3) does not hold for the set of dynamo models.

In Fig. 3c the available energy flux is scaled in such a way that it becomes proportional to the ratio of the flux Rayleigh number divided by the critical Rayleigh number Ra_c (assuming $Ra_c \propto \mathrm{E}^{-4/3}$ and ignoring the influence of Pr on Ra_c). This way of non-dimensionalization is the least susceptible for creating a spurious correlation, because it leads to the smallest spread in the data. Finally, the scheme used in Fig. 3d makes the non-dimensional available flux equivalent to the 'energy flux number' Φ, proposed by Stevenson (1984). Stevenson suggested that a change of regime occurs around $\Phi = 3000$ (or $\Phi^{2/3} \approx 200$; note that $\Phi^{2/3}$ is plotted in Fig. 3d), with $\Lambda \approx 0.003\Phi$ at small Φ and $\Lambda \approx 1$ at large Φ. No indication for a regime change is found. Rule #4 (Table 1), which is supposed to be applicable at low flux, is equivalent to a simple linear dependence of magnetic energy on the available flux when they are normalized using the magnetic scaling (Fig. 3a). Although the best-fitting exponent of 0.70 is slightly larger than 2/3, an exponent of one is not compatible with the results.

So far, we rejected rules #3, 4 and 8 as incompatible with the numerical data. Rule #2 corresponds to a constant value of magnetic energy in the magnetic scaling, but this actually varies by four orders of magnitude (Fig. 3a). Rule #5 predicts a slope of 1/3 in the rotational scaling, which is clearly far off (Fig. 2). Rule #6 is equivalent to the constancy of dimensionless magnetic energy when scaled with $(p, q, r, s) = (3/2,0,1/2,0)$, but this is found to vary within a range of 250. The problem with rule #7 is that is contains a hidden length scale ℓ_α, being the constant of proportionality between the α-parameter in the turbulent mean-field theory used by Sano (1993) and Ω, and which should be added on the right-hand side of rule #7. Sano assumes a fixed value of ℓ_α for the various planets, but the fundamental MHD equations do not support the existence of another length scale that is independent from the other properties. Assuming $\ell_\alpha \propto R_c$ leads of course to rule #2. In summary, we find that all scaling rules listed in Table 1 are incompatible with the numerical dynamo results, with the exception of #9. That is no surprise, since this rule as been suggested on the basis of numerical data in the first place.

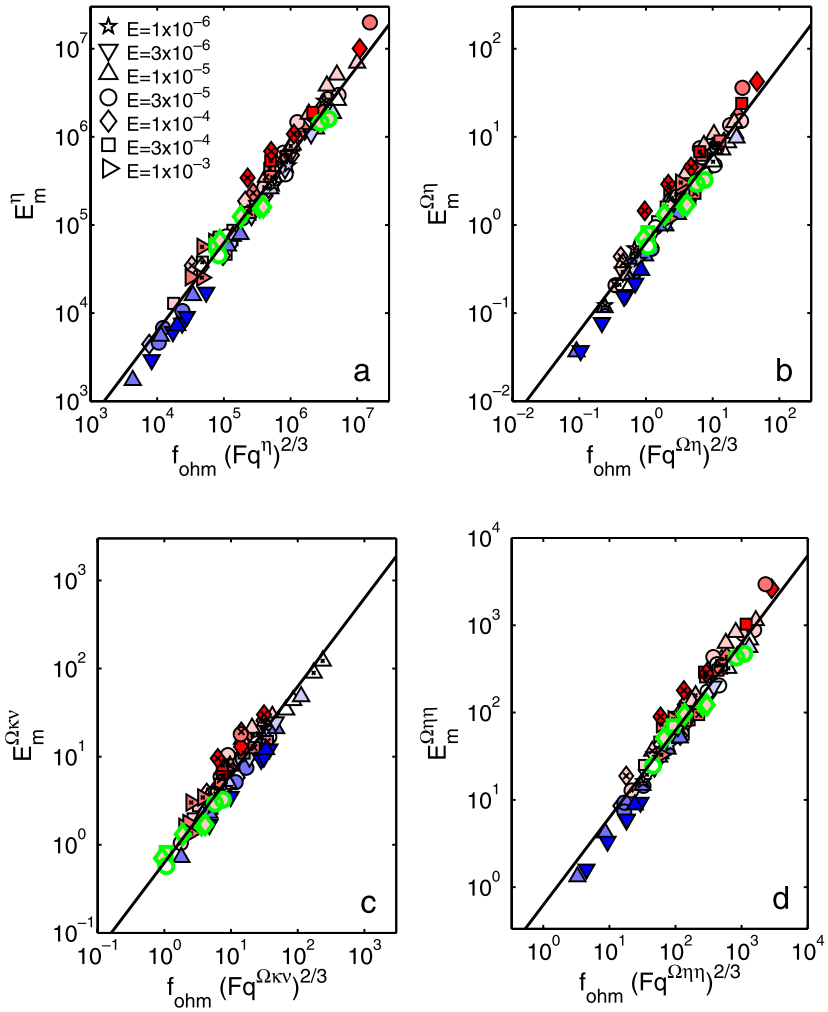

Fig. 3 Magnetic energy versus available power for dynamo models with dipole-dominated fields using different non-dimensionalization schemes. The exponents (p, q, r, s) in the scale values of magnetic energy and the convected flux are in (**a**) $(0, 0, 2, 0)$, in (**b**) $(1, 0, 1, 0)$, in (**c**) $(8/9, -2/9, 0, 4/3)$ and in (**d**) $(2/3, 0, 4/3, 0)$. See Fig. 1 for explanation of symbols

3.3 Field Topology and Reversals

Simply speaking, the numerical dynamos can be classified into those that generate a dipole dominated magnetic field and those with a multipolar field. We use the ratio of the mean dipole field strength at the surface of the dynamo to the combined field strength in harmonic degrees from 1 to 12 as measure for the degree of dipolarity. For the present geomagnetic field, this ratio is 0.65 based on the POMME model (Maus et al. 2006). Christensen and Aubert (2006) proposed that the dipolarity is controlled by a local Rossby number

$$Ro_\ell = \frac{U}{\Omega \ell}, \tag{27}$$

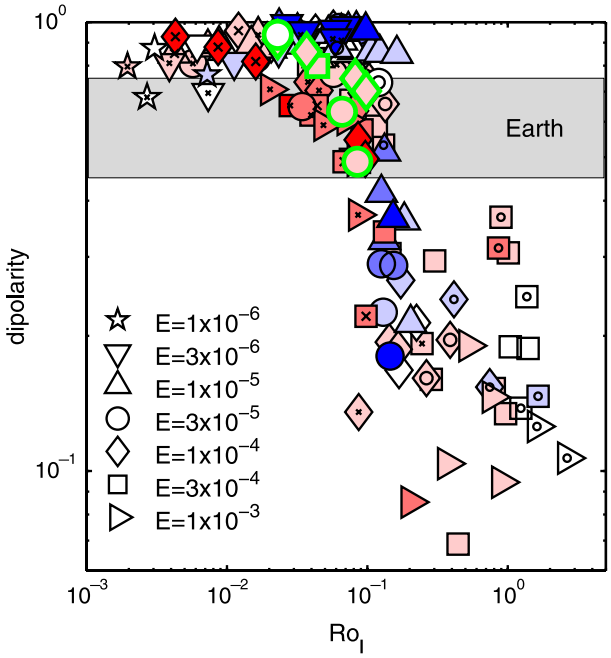

Fig. 4 Degree of dipolarity versus the local Rossby number. See Fig. 1 for explanation of symbols. The likely range for the dipolarity of the geodynamo outside times of reversals and excursions of 0.45–0.75 is marked in grey

where the characteristic length scale ℓ of the flow is derived from the kinetic energy spectrum. Ro_ℓ seems a more appropriate measure for the ratio of inertial forces to the Coriolis force than the Rossby number defined with the global length scale. Sreenivasan and Jones (2006) showed that dynamo models become less dipolar when inertial forces become stronger relative to the Coriolis force. Christensen and Aubert (2006) found in their models that the transition from dipole-dominated dynamos to multipolar dynamos occurs at a critical local Rossby number of 0.12, irrespective of the values of the Ekman number and the Prandtl numbers. An updated version of their diagram is shown in Fig. 4.

Olson and Christensen (2006) confirmed the local Rossby number criterion for the selection of the magnetic field morphology, including also dynamo simulations from the literature. They observed that numerical dynamos that are dipole dominated but show occasional field reversals are only found in the range 0.06–0.12 for Ro_ℓ, i.e. close to the transition point to multipolar dynamos. Wicht et al. (2009) put the range for Earth-like reversal behaviour at slightly higher values of Ro_ℓ. In order to express the local Rossby number in terms of the fundamental control parameters, Olson and Christensen (2006) found it necessary to invoke a dependence on all four parameters. Their suggested scaling law is written here in terms of the non-dimensional available energy flux

$$Ro_\ell = 0.11(Fq^*)^{1/2}E^{-1/3}Pr^{1/5}Pm^{-1/5}. \tag{28}$$

It provides a good fit to the numerical data, but is (so far) purely empirical without an obvious theoretical explanation. Dynamos with different thermal boundary conditions or source-sink distributions may have different values for the critical local Rossby number (Olson and Christensen 2006; Aubert et al. 2009). In dynamo models with stress-free boundaries Simitev and Busse (2005) found a variety of magnetic field pattern; whether their selection is also governed by the value of Ro_ℓ is not clear.

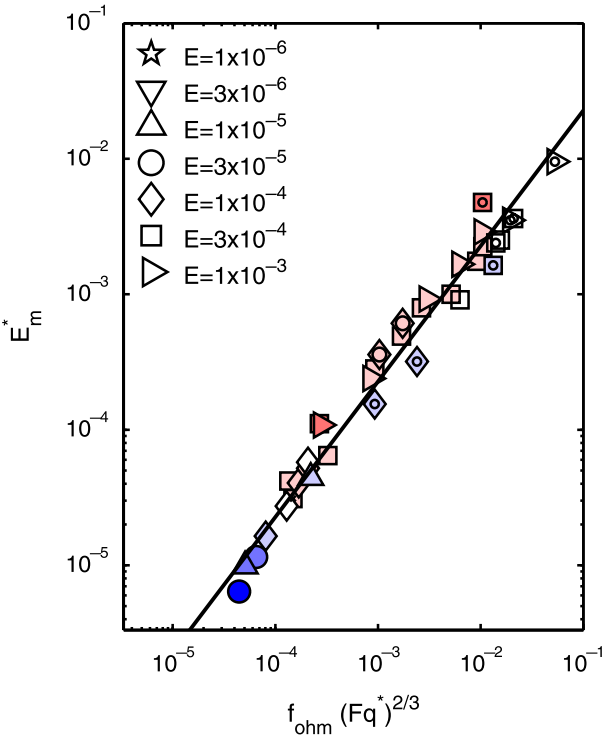

Fig. 5 Non-dimensional magnetic energy density versus 2/3 power of available energy for dynamos generating a multipolar magnetic field. See Fig. 1 for explanation of symbols

3.4 Field Scaling for Multipolar Dynamos

So far, the magnetic field scaling law in Eq. 11 has been tested only for numerical dynamos in the dipole dominated regime. The scaling arguments made in Sect. 2.3 should in principle apply independent of the magnetic field topology. In fact, plotting magnetic energy density against the available flux for the subgroup of multipolar numerical dynamos (dipolarity <0.35) shows again good agreement with the 2/3-power law (Fig. 5). The prefactor c is significantly lower than in case of the dipolar dynamos, 0.23 instead of 0.63. Such difference can be expected because of the different magnetic power spectra. In the non-dipolar case a relatively smaller fraction of the total magnetic energy resides in large spatial scales that hardly contribute to dissipation, therefore at the same value of the magnetic Reynolds number the ohmic dissipation is larger in the multipolar case.

3.5 Scaling of Ohmic Dissipation

Christensen and Tilgner (2004) used a set of numerical dynamo models to derive a scaling law for the ohmic dissipation time τ_λ. An inverse dependence on the magnetic Reynolds number, $\tau_\lambda = 0.27 D^2/\lambda Rm^{-1}$, provides a decent fit to their numerical results. They also found that the fit could be improved by invoking an additional dependence on the magnetic Prandtl number Pm (or, equivalently, on the hydrodynamic Reynolds number). However, they rejected the latter because including results for the ohmic dissipation in the Karlsruhe dynamo experiment supported a simple dependence on Rm alone.

Here we revisit the scaling law for the ohmic dissipation time using the now much larger data basis of numerical dynamo results. A fit of the normalized dissipation time

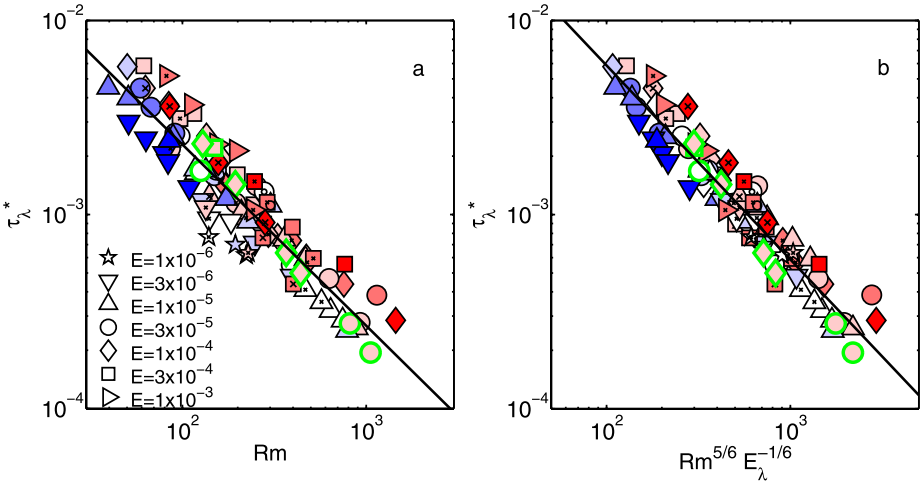

Fig. 6 Fit for ohmic dissipation time (scaled by D^2/λ), (**a**) against magnetic Reynolds number, (**b**) against a combination of magnetic Reynolds number and magnetic Ekman number. Slope -0.93 in (**a**) and -1.0 in (**b**). Symbols as in Fig. 1

$\tau_\lambda^* = \lambda/D^2\tau_\lambda$ versus Rm results in a slightly different exponent of -0.93. Also the standard error of the fit (0.29 with respect to fitting $\ln\tau_\lambda^*$ vs. $\ln Rm$) has increased compared to the original analysis (Fig. 6a). Three different options for a two-parameter fit are tested. Including Pm improves the fit marginally (standard error 0.25). Using the Ekman number as second parameter, the misfit is reduced to 0.17. However, here we concentrate on the magnetic Ekman number $E_\lambda = E/Pm$ as additional parameter, which does not lead to quite the same variance reduction, but still improves the fit (Fig. 6b). It is given by

$$\tau_\lambda^* = 0.59 Rm^{-5/6} E_\lambda^{1/6}, \tag{29}$$

with a standard error of 0.21.

Replacing the dependence of dissipation time on Rm^{-1} with that given by Eq. 29, whose dimensional form is

$$\tau_\lambda = \ell_B^2/\lambda \propto (D/U)^{5/6}\Omega^{-1/6}, \tag{30}$$

reconciles the discrepancy between the exponents found from the numerical data fit for the velocity and the magnetic field, respectively. Using Eqs. 9 and 30 together with the velocity from the CIA-balance (Eq. 7) exactly recovers the 2/3-power law for the magnetic field with its independence from Ω (Eq. 11). The weak dependence on rotating rate in Eq. 30 is plausible, at least for in the numerical models with $Pm \approx 1$. More rapid rotation leads to smaller flow scales in the dynamo (Takahashi et al. 2008). A more small-scaled flow pattern can be expected to be more efficient in generating a small-scaled magnetic field than a large-scaled flow at the same value of Rm. Whether the same argument applies to real planetary dynamos with $Pm \ll 1$ is less clear, because here the smallest scales in the flow do not affect the magnetic field, which is homogenized at these scales by the large magnetic diffusivity.

3.6 Strength of The External Field

Equation 24 predicts the rms magnetic field strength inside the dynamo. But only the long-wavelength part of the magnetic field at the top of the dynamo can be inferred directly from

observations. For planets other than Earth only the dipole and the lowest-order multipoles are known. Olson and Christensen (2006) tested an equivalent rule to Eq. 24 for the rms-strength of the dipole component of the field on the outer boundary and found a decent agreement for dynamo models in the dipolar regime ($Ro_\ell < 0.12$), although the scatter is larger it is than it is for the internal field. In the multipolar regime the scatter becomes very large.

Some earlier theories for the geodynamo assumed that the toroidal component of the magnetic field in the dynamo, which is invisible from the outside, might me much stronger than the poloidal field, similar to what is assumed for the solar dynamo. If this were correct, it would be very difficult to compare scaling law predictions for the internal dynamo field with the observable part of the field. However, all numerical geodynamo models show roughly equal strength of the poloidal and toroidal field components. Therefore, we assume here that the ratios between the internal (poloidal plus toroidal) field and the poloidal outside field found in geodynamo models are representative for planetary dynamos.

The ratio of the rms internal field strength to the dipole strength on the outer boundary has been found in the range between 3 and 10 for dipolar dynamos with a fixed ΔT (Christensen and Aubert 2006). The ratio between internal field strength to the total dynamo surface field strength is around 3.5. However, dynamo models with different thermal boundary conditions and those with a stably stratified layer at the top can have larger ratios between internal field and external dipole field (Aubert et al. 2009; Christensen et al. 2009). The uncertainty in this factor may preclude in some cases a meaningful test of the scaling law based on the observed planetary magnetic field.

3.7 Secular Variation Time Scales

Christensen and Tilgner (2004) used geodynamo models to determine the parameter dependence of the characteristic time scales of secular variation. For the field at a given harmonic degree n, it is defined as the ratio between the degree power of the field and of its time derivative: $\tau_n^{sec} = (B_n^2/\dot{B}_n^2)^{1/2}$. In the models, $\tau_n^{sec} = \tau^{sec}/n$ fits the spectral dependence well for $n > 1$. In the recent geomagnetic field a somewhat steeper decrease on τ_n^{sec} with n has been found (Holme and Olson 2006). For the master coefficient τ^{sec} Christensen and Tilgner (2004) determine an inverse dependence on the magnetic Reynolds number from fitting the numerical data, which is rewritten here as

$$\tau^{sec} = 3.4 \frac{D^2}{\lambda} Rm^{-1} = 3.4 \frac{D}{U}. \tag{31}$$

3.8 Heat Transport

With respect to planetary dynamos, knowing the dependence of the Nusselt number Nu on the Rayleigh number Ra (or on Fq^*) is of limited practical interest, because it is hardly possible to quantify from observation the tiny superadiabatic temperature contrast that drives convection. However, the scaling law for the Nusselt number, $Nu \propto Ra^\beta$, is of great theoretical interest in convection theory. A possible break in slope β is indicative of a change in the dynamical regime, with likely consequences for magnetic field generation in case of a dynamo.

Christensen (2002) and Christensen and Aubert (2006) found for rotating convection and for dynamos a value β of the order 6/5, surprisingly large compared to the well-established value $\beta = 2/7$ in non-rotating turbulent convection. King et al. (2009) showed for rotating convection that the large value of β applies only when the rotational constraints on the

flow are strong and the Ekman boundary layer is thinner than the thermal boundary layer. Above a transition value for the Rayleigh number, $Ra_t = 1.4E^{-7/4}$, the slope of Nu vs. Ra approaches the classical $2/7$ value. They estimated that in the Earth's core Ra is close to Ra_t. The same break in slope occurs in convective dynamo models (E. King, J. Aurnou, personal communications) and is more or less coincident with the change from dipolar to multipolar dynamos. Whether the criterion of the local Rossby number (Sect. 3.3) or that of the transitional Rayleigh number better captures the change in magnetic field geometry remains to be determined.

4 Application to the Planets

4.1 Magnetic Field Strength of Solar System Planets

The only rule that passes the test against numerical model results is Eq. 15, which predicts a dependence of the magnetic field strength on the cubic root of the available power and its independence from the rotation rate. But we face several problems when we want to test the scaling rule against observational data.

We need to know the convected heat flux in the dynamo. The core heat flow can be estimated for Earth within a factor of three (Lay et al. 2008) and for the gas planets it can be deduced from the planet's excess infrared radiation (e.g. Ingersoll et al. 1975). For other terrestrial planets and for Ganymede only crude estimates based on thermal evolution models are available. In these planets the core heat flow is controlled by the sluggish solid state convection in the overlying silicate mantle. The removal of internal heat is more efficient in the presence of plate tectonics compared to cases where mantle convection occurs below a rigid lid. Furthermore, only the convected part of the heat flux is relevant. The fraction of heat that is conducted along an adiabatic temperature gradient must be deducted from the total heat flow. For the gas planets this is not an important issue, but in the terrestrial planets the conducted heat flux is a significant part of the total flux. In some planets it may actually be the only means of heat transport. When a growing solid inner core exists, compositional driving of convection must be accounted for. This can be done by using buoyancy flux instead of the convected heat flux, where the former may have a thermal and a compositional contribution.

Our scaling rule predicts the mean field strength inside the dynamo, but only the field at or above the planetary surface is accessible to observation. The ratios between the internal field and the exterior magnetic field found in numerical dynamo models serve as a guide, but this is fraught with some uncertainty. Also, the scaling law has been tested for a geometry and distribution of buoyancy forces appropriate for the present geodynamo, i.e. a deep fully convecting spherical shell, with a strong flux of buoyancy emanating from the inner core. Other planetary dynamos may operate in a different way, i.e. in a thin shell, with a different distribution of buoyancy sources, and possibly below or above a stably stratified fluid layer. As long as the same basic principles of a power-controlled field strength apply to these dynamos, the efficiency factor as calculated by Eq. 14 should take care of such modifications. However, the spatial spectrum of the magnetic field and the factor relating internal field strength to exterior field strength can be different for the different types of dynamos (Aubert et al. 2009).

Jupiter's magnetic field and the geomagnetic field are similar in terms of the dipole tilt and the ratio between dipole power and the power in low-degree multipoles, suggesting that the dynamos in the two planets are generically similar. Christensen and Aubert (2006)

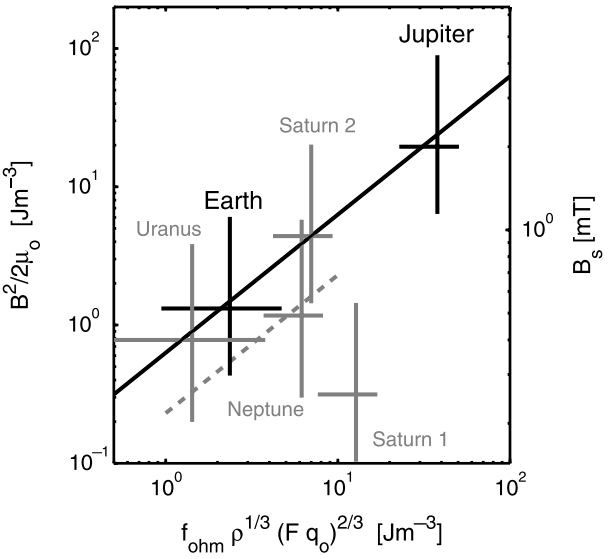

Fig. 7 Magnetic energy density in planetary dynamos vs. the 2/3-power of the available heat flux. The solid line is the prediction of Eq. 15, with $c = 0.63$ taken from the fit to dipolar numerical dynamos, the broken line has $c = 0.23$ found for multipolar dynamos. The equivalent total field strength at the top of the dynamo is plotted on the axis to the right. See text for explanations of the two Saturn cases. Mercury and Ganymede are not included because of the available energy flux is not observationally constrained

and, in a more refined analysis including a detailed calculation of the efficiency factor F, Christensen et al. (2009) compared the predictions of Eq. 15 with the observed fields of Earth and Jupiter. For Earth $F = 0.27 - 0.52$ and for Jupiter $F = 1.1$ is found. In Fig. 7 their result is reproduced, along with estimates for other solar system planets. The internal field strengths deduced from the surface fields of Earth and Jupiter match the predictions well (see Christensen et al. 2009, including online supplementary information for assumptions and error estimates).

For other solar system planets the compliance with our preferred scaling rule is much less clear. But this is also true for the Elsasser number rule, which works well for Earth and Jupiter, but fails for Mercury, Uranus, Neptune (Stevenson 2003), and perhaps marginally for Saturn. We will now discuss these planets one by one.

Mercury's field is enigmatically weak. The heat flow from the core is unknown, but explaining the weak external field on the basis of Eq. 15 by an extremely low energy flux would not be a viable option. The corresponding velocity, obtained via Eq. 7, would imply a subcritical magnetic Reynolds number. Mercury's dynamo may be very different from the geodynamo (Stanley and Glatzmaier 2009, this issue). For example, it may be restricted to a thin fluid shell and generate a strong (hidden) toroidal field, but a weak (observable) poloidal field (Stanley et al. 2005). In the model of Christensen (2006) the dynamo operates in a deep convecting sublayer covered by a thick stagnant fluid region, which arises because the heat flux at Mercury's core-mantle boundary is probably significantly lower than the flux that can be conducted along an adiabatic temperature gradient. Both models could explain the weak field observed outside the planet. At the same time the strength of the internal magnetic fields may comply with the scaling rule of the available energy flux, although this would be very difficult to verify since most of the dynamo field is hidden from observation.

Venus and *Mars* have no active dynamo at present. The heat flow in these planets is probably significantly less than it is in the Earth because of a lack of plate tectonics. In particular, the heat flow in the core may be less than the flux that can be conducted down the adiabatic gradient, so that the core would be thermally stable. The convected heat flow q_c is then zero. In contrasts to Mercury, these planets may have failed to nucleate an inner core. Compositional convection is then unavailable and no dynamo exists. In Mars the early

dynamo, whose existence is suggested by the strong magnetization of the martian crust in the southern hemisphere, would have been powered by a superadiabatic core heat flux during the first couple of hundred million years of the planet's history.

Saturn is similar to Jupiter in its internal structure, which comprises a large core region of metallic hydrogen (Fortney and Nettelmann 2009, this issue). It also has a high internal heat flow. But Saturn's magnetic field is extremely axisymmetric and 20 times weaker than Jupiter's field at the surface. Assuming the top of the dynamo region at a pressure of 1.3 Mbar, which corresponds to $R_c = 0.62R_p$, the scaling rule significantly overpredicts the observed field strength (Fig. 7, Saturn 1). To explain the unexpectedly high heat flux compared to the prediction of evolution models, Stevenson (1980) proposed that at the top of the metallic hydrogen region helium becomes immiscible and precipitates, creating a compositionally stratified layer. Differential rotation in such a convectively stable electrically conducting layer above the dynamo would filter out non-axisymmetric magnetic field components (Stevenson 1982; Christensen and Wicht 2007) and can explain the geometry of Saturn's external field. The thickness of the stably stratified layer, if it exists, is highly uncertain. A deeper dynamo means a lower effective energy flux and, for geometrical reasons, a stronger field at the top of the dynamo for a given surface field. By tuning the upper boundary of the active dynamo region to $R_c = 0.40R_p$, Saturn can be brought to agreement with the theoretical prediction (Saturn 2 in Fig. 7).

In *Uranus* and *Neptune* the dynamo resides in a fluid region of 'ices' that extends to $R_c \approx 0.75R_p$ and has an ionic electrical conductivity (Fortney and Nettelmann 2009, this issue). The magnetic fields of the two planets are similar, with nearly Earth's field strength at the planetary surface, strong dipole tilt, and quadrupole and octupole components that are comparable in strength to the dipole (Russell and Dougherty 2009, this issue). But differences exist for the internal heat flow; for Neptune it is $q_o = 430 \pm 46$ mW m^{-2}, whereas for Uranus it is only 42 ± 47 mW m^{-2} (Peale and Conrath 1991). In the case of Uranus, zero heat flux is within the error bar, but is not compatible with the existence of a convective dynamo. Estimating the internal field strength is difficult, because at the top of the dynamo the quadrupole and octupole components are stronger than the dipole. For the estimates used in Fig. 7 the field models by Holme and Bloxham (1996) are downward continued to R_c. As a rough guide, the total field strength at the dynamo surface is taken to be five times the typical strength in harmonics such as $n = 2$, 3 or 4. This ratio is found in multipolar dynamo models at values of the magnetic Reynolds appropriate for Uranus and Neptune (see below). A mean field strength of 0.4–0.5 mT at the top of the dynamo is inferred and is scaled up by a factor of 3.5 to arrive at the interior field strength. Setting the F-factor to one, the estimated internal field strength is in fair agreement with the theoretical prediction within the uncertainties (Fig. 7). However, the interior of Uranus and Neptune may in part be stably stratified (Hubbard et al. 1995), and host thin-shell dynamos quite unlike the geodynamo (Stanley and Bloxham 2004), which adds to the other uncertainties.

Ganymede's dynamo requires that the small iron core is convecting at present. Estimates of the available energy flux are highly uncertain. Nonetheless, applying the power-based scaling rule, Hauck et al. (2006) showed that plausible estimates for the buoyancy flux lead to a magnetic field strength in agreement with observation.

4.2 Comparison with Magnetic Fields of Rapidly Rotating Stars

The test of the energy flux scaling vis-à-vis the observed planetary field strength is only partly successful. Earth and Jupiter fit well, but for the other planets the uncertainties are large, or particular assumptions must be made that are plausible, but not based on hard

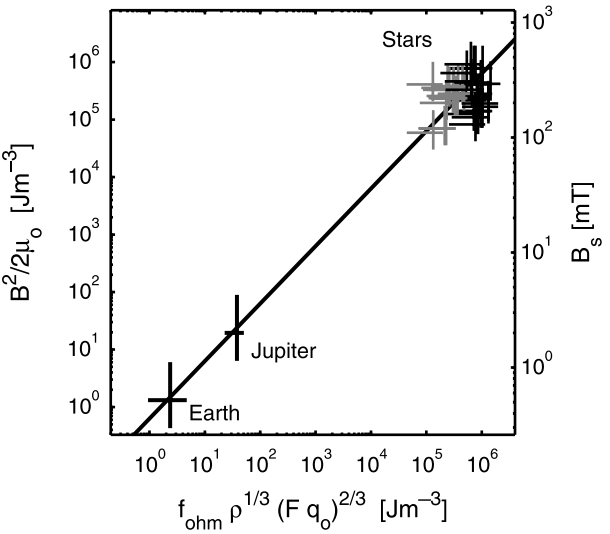

Fig. 8 Similar to Fig. 7 but including rapidly rotating stars main-sequence stars in black and T Tauri stars in grey

constraints. From this comparison alone, it could hardly be claimed the energy flux scaling is superior to the Elsasser number rule. The unsatisfactory situation can be alleviated by including into the comparison other cosmic objects with spherical shell convection-driven dynamos. The solar dynamo is probably too different from planetary dynamos to lend itself to a direct comparison, because much of the field generation is thought to occur at the intense shear layer (tachocline) at the bottom of the solar convection zone. Also, in the slowly rotating Sun Coriolis forces play less of a role than in planetary dynamos (Jones et al. 2009, this issue). Christensen et al. (2009) considered two groups of stars, whose surface magnetic field has been determined spectroscopically through the Zeeman effect. One are low-mass main-sequence stars and the other are very young contracting (T Tauri) stars, with rotation periods of less than 4 days. These objects are fully convective and lack a tachocline (or are nearly fully convective). The energy flux and the magnetic field strength is much larger than it is for planets, yet, the stars seem to follow exactly the same scaling rule as the Earth and Jupiter (Fig. 8). We note that the bold line in Fig. 8 is *not* a fit to the observations, but the slope and the prefactor are derived from theory and numerical models.

4.3 Flow Velocity, Secular Variation and Ohmic Dissipation

The dimensional version of Eq. 22, with an exponent of 2/5 and the prefactor derived from the models inserted, is

$$U = 1.05(Fq_o/\rho)^{2/5}(\Omega R_c)^{-1/5}. \tag{32}$$

Assuming for *Earth's* core an effective superadiabatic heat flux of at the core-mantle boundary of 100 mW m^{-2}, the predicted velocity is ≈ 2 mm s^{-1} (the effective heat flux comprises also compositional driving of the dynamo Christensen et al. 2009). For $\lambda = 1.3$ m^2 s^{-1} this corresponds to a magnetic Reynolds number of 3500, somewhat high compared to other estimates. Using the observed secular variation time of the geomagnetic field $\tau^{sec} \approx 500$ yr in Eq. 31 provides a handle to derive the characteristic velocity in the Earth's core independent of assumptions that enter into inversion models for the flow at the top of Earth's core

(Holme 2007). The result, 0.5 mm s^{-1} or $Rm \approx 800$, is similar to estimates obtained from core flow models. The discrepancy between the two velocity estimates could be resolved by a slightly larger exponent than 2/5 in Eq. 21; a value of 0.45 would be marginally consistent with the data in Fig. 1 and lead to a predicted $U \approx 1$ mm s^{-1}. Also, the energy flux in Earth's core could be significantly smaller than the value assumed above. Christensen and Aubert (2006) had argued for a rather small buoyancy flux (energy flux), using the 'observed' velocity at the top of the core and solving Eq. 32 for Fq_o. The predicted magnetic field strength for a low energy flux dynamo may still be compatible within the uncertainties (but see also Aubert et al. 2009, for a discussions of high-energy and low-energy scenarios).

The amount of ohmic dissipation in the Earth's core has been a contentious issue, with estimates ranging between 0.1 and 3.5 TW (Buffett 2002; Roberts et al. 2003; Labrosse 2003; Gubbins et al. 2003; Christensen and Tilgner 2004). We note that according to our favoured scaling theory for the field strength, the ohmic dissipation is simply related to the available energy flux by $D = f_{ohm} F q_o$. With the range for Fq_o considered in Christensen et al. (2009) and setting $f_{ohm} = 0.75 - 1$, the ohmic dissipation is between 1.1 and 15 TW. This is rather large compared to previous estimates, and in contrast to the range of 0.2–0.5 TW obtained by Christensen and Tilgner (2004) on the basis of the scaling law for the ohmic dissipation time with the inverse magnetic Reynolds number. The revised scaling for τ_λ (Eq. 29) leads, at the same $Rm \approx 800$ as considered in Christensen and Tilgner (2004) and for an Earth-like value of the magnetic Ekman number, to a dissipation time that is five times shorter (five times higher dissipation). This brings the dissipation back in line with the above estimate at a low available energy flux. High energy flux goes along with a higher value of Rm, as discussed before, which shortens the dissipation time further.

In *Jupiter* and *Saturn* the predicted velocities are in the range 10–20 mm s^{-1}. Assuming $\lambda \approx 4$ m^2 s^{-1}, the magnetic Reynolds number is of order 10^5. Secular variations have not been observed at other planets, except that Russell et al. (2001) reported a change of the tilt of Jupiter's dipole by 0.5° over 25 yrs, i.e., at a rate comparable to that of Earth's dipole. Because both the size of the dynamo and the predicted characteristic velocity are an order of magnitude larger in Jupiter compared to the geodynamo, the secular variation time scales should in fact be the same according to Eq. 31. NASA's Juno mission may constrain the secular variation of Jupiter's field in the future.

For *Uranus* and *Neptune* the predicted velocities are 3 mm s^{-1} and 8 mm s^{-1}, respectively. For $\lambda \approx 400$ $m^2 s^{-1}$ (Nellis et al. 1988) and a deep convection shell with $D \approx 13{,}000$ km, the respective magnetic Reynolds numbers are 110 and 300. This is not very far above the critical value for the onset of dynamo action of about 50. Assuming that convection is restricted to a thin shell overlying a stably stratified interior might bring Rm dangerously close to the critical value, in particular for Uranus.

4.4 Field Topology and Reversals

Using Eq. 28, Olson and Christensen (2006) made a crude estimate for the local Rossby number in the different planets. For Earth the predicted value is 0.1, i.e. close to the transition between the dipolar and multipolar regime and in a range where occasional dipole reversals have been found in numerical models. But while the predictions seems to agree well with the known behaviour of the geomagnetic field, there is a problem with such high value of Ro_ℓ. The associated length scale ℓ is only 100 m—we note that it is less than the length scale of a few kilometers predicted by the CIA-balance (Eq. 8). Even if the flow in the Earth's core carried significant energy in 100-m-sized eddies, it is difficult to understand how they could affect the magnetic field, which is homogenized by diffusion at such small scales. A possible

mechanism is a strong back-reaction of the small eddies on the circulation at larger scales through Reynolds stress (inertial) effects. This is typical in rotating convection and leads, for example, to the excitation of vigorous zonal jet flow.

For the gas planets, and in particular for Uranus and Neptune, Olson and Christensen (2006) estimated values of Ro_ℓ an order of magnitude smaller than for the Earth's core. Hence one would expect an axially dipolar magnetic field at Uranus and Neptune, which is in obvious contrast to the strong dipole tilt and large quadrupole and octupole contributions. A thin shell dynamo above a stably stratified conducting core might explain the multipolar nature of the magnetic field (Stanley and Bloxham 2004, 2006), but it could run into the problem of a subcritical magnetic Reynolds number, as mentioned above. Only for Mercury a local Rossby number larger than one is expected because of its slow rotation, which puts Mercury into the multipolar dynamo regime. The existence of a multipolar field inside Mercury's dynamo, despite the dipole dominance of the field at Mercury's surface, plays in fact an essential role in the model by Christensen (2006) to explain the low external dipole moment.

So far, the support for the rule of the local Rossby number as criterion for the selection of the magnetic field topology is rather scanty from the comparison with the planets. It must also be kept in mind that the rule for calculating Ro_ℓ (Eq. 28) is purely empirical, obtained by fitting model data, and that it requires huge extrapolations to apply it to the planets. However, some support for the validity of the rule comes again from studying the magnetic fields of low-mass stars. Mapping the field of several such stars by a technique called Zeeman-Doppler tomography, Donati et al. (2008) found a trend from multipolar to axially dipolar geometry when the Rossby number (defined in a somewhat analogous to the local Rossby number used here) becomes smaller.

5 Discussion and Outlook

In the past, scaling laws for planetary dynamos have been suggested on the basis of fairly general theoretical principles. In recent years, it has become possible to compare scaling laws with the results of direct numerical simulations of the dynamo. One apprehension has been that these dynamo models, running at parameter values vastly different from planetary dynamos, might be in a different dynamical regime and in particular being strongly influenced by viscosity. But this fear seems to be unfounded—if it were true the scaling for the Rossby number and the non-dimensional magnetic field strength in the models should depend on the Ekman number, but no such dependence is found. A concern that must be taken more seriously is that the numerical simulations assume a magnetic Prandtl number of order one, whereas the planetary value is of order 10^{-6}. The disparity of the small length scales in the flow and small scales of the magnetic field, which exists in planetary dynamos, is not accounted for in the models. There are hints in the numerical data for an influence of the magnetic Prandtl number on the velocity and magnetic field scaling laws (Christensen and Aubert 2006). The dependence on Pm is weak, but because of the large range over which the magnetic Prandtl number must be extrapolated, it would lead to significant differences if it persisted to very low values of Pm. From this point of view, it seems more urgent to develop dynamo models at low magnetic Prandtl number than models with a very low Ekman number. But the tasks are not independent—to obtain a dipolar dynamo model at low Pm, the Ekman number must also be made very small. Otherwise the strong driving of the flow, which is required in a low-Pm dynamo, would lead to a dominance of inertial forces and to a multipolar magnetic field (Christensen and Aubert 2006). Truely low magnetic Prandtl

numbers will be hard to reach in numerical simulations, and insights may come from future laboratory dynamo experiments with significant net rotation.

The agreement of the energy-flux based magnetic field scaling law with the numerical results (Figs. 2 and 3), and its agreement with observation for objects with presumably simple dynamos (Fig. 8), provide rather strong support for its validity (simple dynamos are those operating in deep convective layers without shielding by stagnant regions). The magnetic field strength does not seem to be controlled by a force balance, but rather by the energetics of the planet (or star). This does not mean that the flow in the dynamo would not obey a balance in which Lorentz forces, Coriolis forces and buoyancy forces play an important role. But the force balance may be more subtle than what is assumed in simple scaling arguments. For example, pressure gradients could cancel most of the Coriolis force, or magnetic field and velocity could be strongly aligned, so that induction effects are small and $\sigma U B^2$ is an overestimate for the order of the Lorentz force. Also, inertial forces that kick in at small flow scales may be more important than previously assumed.

The rule of the local Rossby number for the selection of the field topology seems to be on less solid ground than the scaling rule for the field strength. On the one hand, the local Rossby number rule is supported by a large number of dynamo simulations and it seems plausible that the ratio of inertial forces to Coriolis forces can have an effect on the magnetic field. On the other hand, it is not understood in detail why strengthening of the inertial force leads to a severe change in the magnetic field configuration. While inertial forces are clearly important in some of the dynamo models, it is not clear how they can become influential in planetary dynamos. Furthermore, the rule for estimating the local Rossby number at planetary parameter values, which are vastly different from model values, is also not beyond doubt. The local Rossby number rule has rather limited support from a comparison of its prediction with natural dynamos. For the two planets with a multipolar field geometry, Uranus and Neptune, the local Rossby number is not larger and probably smaller than for Earth or Jupiter. Nonetheless, so far only the local Rossby number rule has been suggested as a general criterion for the selection of the magnetic field geometry and it can be considered as a viable hypothesis. At any rate, the qualitative statement that more rapid rotation favours dipolar dynamos seems fairly robust.

Further studies are needed into types of planetary dynamos that differ from those in Earth and Jupiter. For dynamos in thin shells, dynamos with a different distribution of buoyancy sources than considered so far, or dynamos with stably stratified layers, the prefactors in the scaling laws or the critical numbers (for Ro_ℓ, Rm) must be determined. While this is amenable to numerical simulations (e.g. Aubert et al. 2009), unfortunately the details of the dynamo structure in Mercury, Saturn, Uranus or Neptune are poorly known. The factors relating the internal field strength to that of the observed external field must also be reevaluated. They could be more variable for multipolar dynamos than for dipolar ones (compare Fig. 4). For these reasons the application of scaling laws to planets with 'special' dynamos may remain tentative.

The scaling law based on energy flux provides a handle for estimates of the strength of Earth's paleofield (Aubert et al. 2009) and for the magnetic fields of now extinct dynamos, for example in early Mars or in large differentiated asteroids (Weiss et al. 2008, 2009, this issue). It also allows to estimate the magnetic field strength of extrasolar planets. For a relatively young supermassive planet of several Jupiter masses, Christensen et al. (2009) obtained a surface field an order of magnitude stronger than Jupiter's field. The strong field would imply a much higher intensity of non-thermal radio emissions than in the case of Jupiter (Zarka 2007). This could lead to the new detection of such planets. From observations of the radiowave frequency spectrum, which has a cutoff at the electron cyclotron frequency near the planet's surface $\omega_c \propto B_P$, the field strength could be determined.

References

J. Aubert, D. Brito, H.C. Nataf, P. Cardin, J.P. Masson, Phys. Earth Planet. Inter. **128**, 51 (2001)
J. Aubert, S. Labrosse, C. Poitou, Geophys. J. Int. (2009, submitted)
D. Breuer, S. Labrosse, T. Spohn, Space Sci. Rev. (2009, this issue)
B.A. Buffett, Geophys. Res. Lett. **29** (2002). doi:1.12029/2001GL014649
F.H. Busse, Phys. Earth Planet. Inter. **12**, 350 (1976)
J.C. Cain, P. Beaumont, W. Holter, Z. Wang, H. Nevanlinna, J. Geophys. Res. **100**, 9439 (1995)
S. Chandrasekhar, *Hydrodynamic and Hydromagnetic Stability* (Oxford University Press, Oxford, 1961)
U.R. Christensen, J. Fluid Mech. **470**, 115 (2002)
U.R. Christensen, Nature **444**, 1056 (2006)
U.R. Christensen, J. Aubert, Geophys. J. Int. **166**, 97 (2006)
U.R. Christensen, V. Holzwarth, A. Reiners, Nature **457**, 167 (2009)
U.R. Christensen, P. Olson, G.A. Glatzmaier, Geophys. J. Int. **138**, 393 (1999)
U.R. Christensen, A. Tilgner, Nature **429**, 169 (2004)
U.R. Christensen, J. Wicht, in *Treatise of Geophysics, vol. 8: Core Dynamics*, ed. by G. Schubert (Elsevier, Amsterdam, 2007), pp. 245–282
S.A. Curtis, N.F. Ness, J. Geophys. Res. **91**, 11003 (1986)
V. Dehant, H. Lammer, Y.N. Kulikov et al., Space Sci. Rev. **129**, 279 (2007)
J.-F. Donati, J. Morin, P. Petit et al., Mon. Not. R. Astron. Soc. **390**, 545 (2008)
J.J. Fortney, N. Nettelmann, Space Sci. Rev. (2009, this issue)
D.J. Galloway, M.R.E. Proctor, N.O. Weiss, J. Fluid Mech. **87**, 243 (1978)
G.A. Glatzmaier, P.H. Roberts, Nature **337**, 203 (1995)
D. Gubbins, D. Alfè, G. Masters, G.D. Price, M.J. Gillan, Geophys. J. Int. **155**, 609 (2003)
D. Gubbins, P. Roberts, in *Geomagnetism, vol. 2*, ed. by J.A. Jacobs (Academic Press, London, 1987), pp. 1–183
S.A. Hauck, J.M. Aurnou, A.J. Dombard, J. Geophys. Res. **111**, E09008 (2006)
R. Holme, in *Treatise of Geophysics, vol. 8: Core Dynamics*, ed. by G. Schubert (Elsevier, Amsterdam, 2007), pp. 107–130
R. Holme, J. Bloxham, J. Geophys. Res. **101**, 2177 (1996)
R. Holme, N. Olson, Geophys. J. Int. **166**, 518 (2006)
W.B. Hubbard, M. Podolak, D.J. Stevenson, in *Neptune and Triton*, ed. by D.P. Cruikshank (University of Arizona Press, Tucson, 1995), pp. 109–138
A.P. Ingersoll, G. Münch, G. Neugebauer et al., Science **188**, 472 (1975)
C.A. Jones, M.J. Thompson, S. Tobias, Space Sci. Rev. (2009, this issue)
E. King, S. Stellmach, J. Noir, U. Hansen, J. Aurnou, Nature **457**, 301 (2009)
R. Kippenhahn, A. Weigert, *Stellar Structure and Evolution* (Springer, Berlin, 1990)
S. Labrosse, Phys. Earth Planet. Inter. **140**, 127 (2003)
T. Lay, J. Hernlund, B.A. Buffett, Nature Geosci. **1**, 25 (2008)
M. Leweling, T. Spohn, Planet. Space Sci. **45**, 1389 (1997)
S. Maus, M. Rother, C. Stolle et al., Geochem. Geophys. Geosys. **7**, Q07008 (2006)
H. Mizutani, T. Yamamoto, A. Fujimura, Adv. Space Res. **12**, 265 (1992)
W.J. Nellis, D.C. Hamilton, N.C. Holmes et al., Science **240**, 779 (1988)
P. Olson, U.R. Christensen, Earth Planet. Sci. Lett. **250**, 561 (2006)
J.C. Peale, B.J. Conrath, J. Geophys. Res. **96**, 18921 (1991) supplement
P.H. Roberts, C.A. Jones, A. Calderwood, in *Earth's Core and Lower Mantle*, ed. by C.A. Jones, A.M. Soward, K. Zhang (Taylor & Francis, London, 2003), pp. 100–129
C.T. Russell, Nature **272**, 147 (1978)
C.T. Russell, M.K. Dougherty, Space Sci. Rev. (2009, this issue)
C.T. Russell, Z.J. Yu, K.K. Khurana, M.G. Kivelson, Adv. Space Res. **28**, 897 (2001)
Y. Sano, J. Geomag. Geoelectr. **45**, 65 (1993)
G. Schubert, M.N. Ross, D.J. Stevenson, T. Spohn, in *Mercury*, ed. by F. Vilas, C.R. Chapman, M.S. Matthews (University of Arizona Press, Tucson, 1988), pp. 651–666
G. Schubert, T. Spohn, J. Geophys. Res. **95**, 14095 (1990)
R. Simitev, F.H. Busse, J. Fluid Mech. **532**, 365 (2005)
B. Sreenivasan, C.A. Jones, Geophys. J. Int. **164**, 467 (2006)
F.D. Stacey, *Physics of the Earth* (Wiley, New York, 1977)
S. Stanley, J. Bloxham, Nature **428**, 151 (2004)
S. Stanley, J. Bloxham, Icarus **184**, 556 (2006)
S. Stanley, J. Bloxham, W.E. Hutchison, Earth Planet. Sci. Lett. **234**, 341 (2005)
S. Stanley, G. Glatzmaier, Space Sci. Rev. (2009, this issue)

S.V. Starchenko, C.A. Jones, Icarus **157**, 426 (2002)
D.J. Stevenson, Geophys. Astrophys. Fluid Dyn. **12**, 139 (1979)
D.J. Stevenson, Science **208**, 746 (1980)
D.J. Stevenson, Geophys. Astrophys. Fluid Dyn. **21**, 113 (1982)
D.J. Stevenson, Rep. Prog. Phys. **46**, 555 (1983)
D.J. Stevenson, Astronom. Nachr. **305**, 257 (1984)
D.J. Stevenson, Earth Planet. Sci. Lett. **208**, 1 (2003)
D.J. Stevenson, T. Spohn, G. Schubert, Icarus **54**, 466 (1983)
F. Takahashi, M. Matsushima, Y. Honkura, Phys. Earth Planet. Inter. **167**, 168 (2008)
B.P. Weiss, J.S. Berdahl, L. Elkins-Tanton et al., Science **322**, 713 (2008)
B.P. Weiss, J. Gattacceca, S. Stanley, P. Rochette, U.R. Christensen, Space Sci. Rev. (2009, this issue)
J. Wicht, A. Tilgner, Space Sci. Rev. (2009, this issue)
J. Wicht, S. Stellmach, H. Harder, in *Geomagnetic Field Variations*, ed. by K.H. Glassmeier, H. Soffel, J.F.W. Negendank (Springer, Berlin, 2009), pp. 107–158
P. Zarka, Planet. Space Sci. **55**, 598 (2007)